

Structure optimization of $\text{YBa}_2\text{Cu}_3\text{O}_7$ and its influence on phonons and Fermi surface

Robert Kouba, Claudia Ambrosch-Draxl, and Bernd Zangger

Institut für Theoretische Physik, Universität Graz, Universitätsplatz 5, A-8010 Graz, Austria

(Received 12 April 1999)

We have optimized the crystal structure of $\text{YBa}_2\text{Cu}_3\text{O}_7$ using the local-density approximation in the framework of density functional theory. By this procedure we find excellent agreement with experimental data for the A_{1g} phonon modes and their pressure dependence. With respect to previous calculations performed for the unrelaxed geometry a considerable part of the outermost Fermi surface sheet is lost. This finding explains why in that region of the Brillouin zone no feature has been detected experimentally. In accordance with measured data the hole pocket around the S point is absent. [S0163-1829(99)04934-6]

Local-density functional (LDA) calculations have been successfully applied to high-temperature superconductors, e.g., $\text{YBa}_2\text{Cu}_3\text{O}_7$, concerning various aspects like structural and vibrational properties¹⁻⁴ and electron density distributions,⁵ as well as optical spectra.⁶⁻⁹ Thus the applicability of the method to the metallic phases within this class of materials seems to be settled. Moreover, it turned out that the strong Coulomb correlations responsible for the overestimation of bandwidths and the incapability of reproducing the antiferromagnetic insulating phases hardly affect the structural and vibrational properties even for the insulating materials.¹⁰

A variety of calculations have, in general, revealed the same results. Looking at the details, however, there are variations due to different methods and approximations, and limited accuracy. This could be significant for several reasons which shall be explained on the basis of some features of $\text{YBa}_2\text{Cu}_3\text{O}_7$: Although most of the electronic structure calculations agree in the overall picture of the band structure,¹¹⁻¹³ they differ in the position and extension of saddle points and in the presence or absence of the fourth Fermi surface sheet (hole pocket). These details could be crucial for the superconducting mechanism, e.g., within the van Hove scenario. Thus it is important to know what are the results of the most accurate calculation and which feature is robust or sensitive to what kind of approximation. Since the Fermi level is the only single-particle energy theoretically fully justified to be interpreted within density functional theory (DFT), the investigation of the Fermi surface is a key feature for DFT calculations. Another example are the A_{1g} phonons where several publications differ by up to 10%, which is also the order of magnitude for the deviation from the experimental values. Although this discrepancy is not huge, it can give rise to speculations about anharmonic effects or the limits for LDA calculations. Since LDA is well known for underestimating the unit cell volumes of transition metals, the use of the experimental lattice parameters represents an inconsistency.¹⁴ Indeed, it turned out that a reduction of the unit cell volume by 3% leads to improved phonon frequencies¹⁵ and changes in the band structure.¹³ In this paper, we show that a consistent LDA calculation provides excellent agreement between theory and experiment for the A_{1g} modes, in terms of frequencies as well as eigenvectors, and for the Fermi surface. Our procedure also allows us to

determine the bulk modulus and the pressure-induced changes in the crystal structure. The measured volume effect on the phonon frequencies is very well reproduced by our calculations. The underestimation of the lattice parameters is not bigger than for materials which are undoubtedly treated within the LDA.

We optimize the lattice parameters a , b , and c of $\text{YBa}_2\text{Cu}_3\text{O}_7$, and the c -axis coordinates of Ba, Cu, O(2), O(3), and O(4). We proceed in two steps: First, adopting the experimental ratios between the three lattice constants, we determine the equilibrium structure by calculating total energy values as a function of the cell volume. Second, by keeping the so found equilibrium volume constant, we optimize the c/a and c/b ratios simultaneously. In both steps, energy changes due to internal strain of the ions are accounted for by evaluating the corresponding atomic forces and letting the ions relax to their respective equilibrium positions. Finally, we determine the influence of this structural optimization on the phonon frequencies and eigenvectors in the A_{1g} symmetry at $q=0$ and we investigate the changes in the Fermi surface.

We perform all-electron band structure calculations using the full-potential linearized augmented plane-wave (FLAPW) method.^{16,17} Our basis set includes approximately 2000 LAPW's. Semicore states (Y $4s$, Y $4p$, Ba $5s$, Ba $5p$, Ba $4d$, Cu $3s$, Cu $3p$, and O $2s$) are treated by supplementing the LAPW's by local orbitals. The Brillouin zone integrations are carried out on a \mathbf{k} -point mesh consisting of 72 points in the irreducible wedge using a Gaussian smearing of 0.002 mRyd. This mesh turned out to be sufficient for total energy studies with respect to the optimization of the cell volume. In order to obtain atomic forces and phonon modes within a very high precision, 243 \mathbf{k} points are used. For convergence studies we repeated our calculations for the theoretical equilibrium structure on a 576- \mathbf{k} -point mesh.

We find the theoretical equilibrium volume 6% ($\pm 0.2\%$) below the experimental value, which is in accordance with previous calculations.^{1,11} The optimized c/a and b/a ratios are 1.25% ($\pm 0.25\%$) and 0.375% ($\pm 0.125\%$) smaller than the experimental data which are $c/a=3.052$ and $b/a=1.016$. The convergence of total energy and force values is better than 10^{-5} Ryd and 10^{-2} mRyd/a.u.², respectively. A comparative listing of structural data for the fully optimized and the purely volume optimized structures (de-

TABLE I. Calculated structural data for the fully optimized (S_{VRP}) lattice parameters, the purely volume-optimized structure (S_{VP}), and the experimental lattice constants (S_P^{expt}) (Ref. 3) compared to experimental data (Ref. 18). The calculated energy differences are taken relative to the S_P^{expt} case.

	S_{VRP}	S_{VP}	S_P^{expt}	S^{expt}
Volume [\AA^3]	163.1	163.1	173.5	173.5
c/a	3.015	3.052	3.052	3.052
b/a	1.012	1.016	1.016	1.016
ΔE [mRyd]	-21.5	-21.2	0	
z_{Ba} [c]	0.1817	0.1816	0.1812	0.1843
$z_{\text{Cu}(2)}$ [c]	0.3507	0.3505	0.3530	0.3556
$z_{\text{O}(2)}$ [c]	0.3765	0.3771	0.3789	0.3773
$z_{\text{O}(3)}$ [c]	0.3770	0.3771	0.3783	0.3789
$z_{\text{O}(4)}$ [c]	0.1619	0.1610	0.1586	0.1584

noted from now on S_{VRP} and S_{VP} , respectively), and the experimental situation (S^{expt}) is displayed in Table I. Additionally, we also provide in the third column the theoretical equilibrium values of the internal coordinates when experimental lattice constants are assumed in the calculation (S_P^{expt}).³ These values are the starting point for our investigation into the interplay between changes in the lattice constants and internal coordinates.

First, comparing the S_{VP} with the S_P^{expt} structure we note that strain related relaxations of ionic positions are most pronounced for O(4) and Cu(2) whereas the Ba position gets merely scaled down along the c axis when reducing the lattice constants. The changes in the O(2) and O(3) positions are such that relative to the respective c axis the buckling to the Cu(2) atom is enhanced and the distance between the Cu-O layers increased. The relative c -axis position of the Cu(2) atom is lowered, while O(4) is shifted upwards, leading to a significant change in the ratio between the O(4)-Cu(2) and O(4)-Cu(1) distances from 1.224 (S_P^{expt}) to 1.177 (S_{VP}). This tendency of altered bond strength with pressure is consistent with experimental investigations¹⁹ and the c -axis strain calculations of Pickett.⁴ With regard to cohesive energies we observe a change of -21.2 mRyd between the two structures. Recalculating the S_{VP} structure assuming the equilibrium positions of the S_P^{expt} structure increases the total energy by only 1.2 mRyd. This indicates that in $\text{YBa}_2\text{Cu}_3\text{O}_7$ relative changes of bond lengths due to volume compression play a subordinate role for the corresponding changes in the total energy.

Second, we compare the S_{VP} structure with the S_{VRP} structure, which both have the same unit cell volume (6% lower than experiment) but differ with respect to lattice parameter ratios and relaxation of atomic positions. The transition from the S_{VP} structure to the S_{VRP} structure causes a decrease of the total energy by 0.3 mRyd. Approximately 50% of this value can be attributed to strain-induced relaxations of the internal coordinates. The other 50% are related to the lowering of the c/a and c/b ratios. The shortening of the c axis again leads to a small decrease in the bond length ratio between O(4)-Cu(2) and O(4)-Cu(1). Additionally, we observe a slight lowering of the O(2) position relative to the compressed c axis.

TABLE II. Phonon frequencies in cm^{-1} for the five A_{1g} modes at $q=0$ calculated for the fully optimized (S_{VRP}) lattice parameters, and for the experimental structure (S_P^{expt}). The data are compared to experimental (S^{expt}) results (Refs. 20–22). Relative deviations are given as percentage with respect to the average experimental values.

	S_{VRP}	S_P^{expt}	S^{expt}
Ba	123 (+4%)	102 (-13%)	116–119
Cu(2)	147 (0%)	127 (-14%)	145–150
O(2)-O(3)	338 (+1%)	317 (-5%)	335–336
O(2)+O(3)	422 (-3%)	387 (-12%)	435–440
O(4)	487 (-2%)	450 (-9%)	493–500

In several works published in the past,^{1–3,11} it has been demonstrated that when fixing the unit cell volume of $\text{YBa}_2\text{Cu}_3\text{O}_7$ at the experimental value the calculated phonon frequencies are up to 10% lower than the experimental ones. It has been argued^{1,3,4} that a considerable part of this discrepancy might be attributed to the structural overbinding effect caused by the LDA. This argument was supported by frozen phonon calculations for a 3% volume reduced crystal¹⁵ where a considerable enhancement of frequency values was already found. In the present work, we determine the dynamical matrix of the A_{1g} phonon modes at $q=0$ for the fully optimized structure. In Table II, the resulting frequencies are compared to experimental values^{20–22} as well as theoretical results for the experimental lattice parameters. The corresponding eigenvectors are listed in Table III. The differences to previous results for the experimental volume³ are due to the refined \mathbf{k} -point mesh used in this work (see above). By reducing the experimental lattice parameters to the theoretical equilibrium structure all five modes are significantly enhanced. The discrepancy with experimental values has vanished. A great part of the enhancement effect (between 60% and 100% for all modes) is already induced by the pure volume optimization. Only for the O(2)-O(3) mode does the ratio optimization additionally increase the frequency by more than 5 cm^{-1} . We also want to stress that the overall hardening of the 500 cm^{-1} by 35 cm^{-1} is particularly noticeable as this effect could not be achieved by employing gradient corrections (GGA's) to the LDA exchange correlation potential.³ With regard to the mode admixture we observe a slightly stronger decoupling of the Ba and Cu vibration in the two lowest-lying modes. The associated diagonal and off-diagonal terms in the dynamical matrix reproduce experimental values very well.²⁰ Focusing on the oxygen-dominated vibrational eigenmodes, we see that the O(2) and O(3) contributions to the 500 cm^{-1} mode have become significantly reduced. Additionally, the coupling constant between Cu and O(4) almost vanishes.

Experimental investigations have revealed that the pressure effect on the frequencies of the three oxygen modes is characterized by positive linear pressure coefficients $d\omega/dp$, which are constant over a wide range of pressure values (up to 12 GPa).²³ For the 500 cm^{-1} mode the value of this quantity was found to be 5.5 $\text{cm}^{-1}/\text{GPa}$, 4.6 $\text{cm}^{-1}/\text{GPa}$ for the 440 cm^{-1} mode, and 3.2 $\text{cm}^{-1}/\text{GPa}$ for the 338 cm^{-1} mode. To compare our calculations to these findings, we use the experimentally determined volume compressibility dV/dP

TABLE III. Eigenvectors for the five A_{1g} modes at $q=0$ calculated for fully optimized lattice parameters (left side) and for the experimental crystal structure, respectively (right side). The sequence of modes is the same as in Table II.

Ba	Cu	O(2)	O(3)	O(4)
0.91/0.84	0.41/0.54	0.05/0.05	0.05/0.05	0.04/−0.01
0.42/0.54	−0.90/−0.83	−0.08/−0.09	−0.06/−0.06	0.00/0.07
0.00/−0.01	0.03/0.04	−0.77/−0.81	0.63/0.59	−0.01/−0.02
0.03/0.02	0.11/0.08	−0.60/−0.50	−0.73/−0.71	−0.31/−0.49
0.02/0.03	−0.02/−0.12	0.19/0.30	0.24/0.38	−0.95/−0.87

(Ref. 19) to translate the pressure coefficients to volume coefficients according to

$$\frac{d\omega}{dV} = \frac{d\omega}{dP} \left(\frac{dV}{dP} \right)^{-1}. \quad (1)$$

The resulting values are $-3.9 \text{ cm}^{-1}/\text{\AA}^3$ (500 cm^{-1} mode), $-3.3 \text{ cm}^{-1}/\text{\AA}^3$ (440 cm^{-1} mode), and $-2.3 \text{ cm}^{-1}/\text{\AA}^3$ (338 cm^{-1} mode), respectively. We obtain $\delta\omega$ from the two sets of frequency values related to the -3% - and -6% -volume-reduced unit cells (where the volume difference corresponds to a pressure of about 6 GPa). The theoretical volume coefficients are now determined to be $-3.7 \text{ cm}^{-1}/\text{\AA}^3$ (500 cm^{-1} mode), $-3.0 \text{ cm}^{-1}/\text{\AA}^3$ (440 cm^{-1} mode), and $-2.6 \text{ cm}^{-1}/\text{\AA}^3$ (338 cm^{-1} mode). These values compare very well to the experimental data.

To our knowledge, no *ab initio* calculation of the bulk modulus B of $\text{YBa}_2\text{Cu}_3\text{O}_7$ has been carried out so far. On the basis of an ionic-crystal model related to experimental data, Ledbetter and Lei²⁴ concluded that the value should be in the range of 107 ± 10 GPa. Experimental studies on a monocrystal using high-pressure x-ray diffraction reported a value for $B = 115$ GPa.²⁵ The values of different experiments, however, range from 27 to 196 GPa.²⁶ We perform total energy calculations for four different volumes in the vicinity of the crystals' theoretical equilibrium structure. To simplify the calculations the c/a and c/b ratios are set to the same values for all four volumes. This procedure is justified by our above

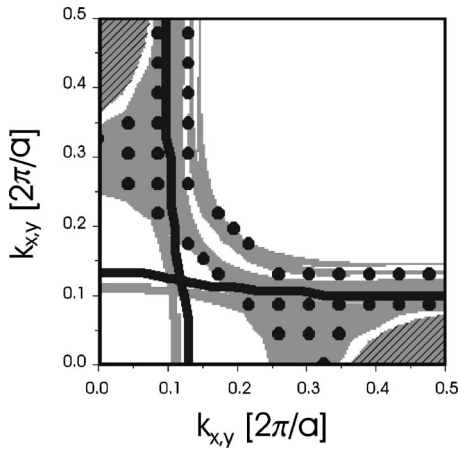


FIG. 1. Projection of the $\text{YBa}_2\text{Cu}_3\text{O}_7$ FS sheets onto the (k_x, k_y) plane (grey area) compared to ARPES data (Ref. 28) (black dots) and ACAD experiments (Ref. 29) (black lines). For comparison the ACAD data as well as the theoretical results are mirrored along the diagonal (see text).

finding that in the course of optimizing lattice parameters the “ratio effect” on changes in the total energy is two orders of magnitude smaller than the “volume effect” (0.3 mRyd compared to ≈ 20 mRyd). The internal ionic parameters are fully optimized for each structural configuration. The resulting energy values are fitted to a polynomial function, whose origin is taken at 6% below the experimental volume. It turns out that anharmonic terms are negligible. We thus obtain a value of $B = 142$ GPa.

Concerning the Fermi surface (FS), a large number of LDA calculations has been carried out starting from the experimentally determined geometry (e.g., Refs. 11–13). It is evident that experiment and theory agree qualitatively. Hereby, one important fact is that different experimental methods probe different features of the electronic structure. Since the positron momentum density turned out to be largest at the copper-oxygen chains,²⁷ two-dimensional (2D) angular correlation of annihilation radiation (ACAR) measurements are most sensitive to the Fermi surface sheet stemming from these structural elements. On the other hand, angle-resolved photoemission spectroscopy (ARPES) data give rise to two FS sheets related to bands formed by the copper-oxygen planes. In Fig. 1, a projection of all three sheets is compared to the experimental findings of Liu *et al.*²⁸ (black dots) and Haghghi *et al.*^{12,29} (black lines). While the latter data have been obtained using untwinned single crystals, the ARPES measurements have been performed on twinned samples. Thus, for comparison, the ACAR data as well as our theoretical results have been mirrored along the diagonal. All these data as well as newer ARPES measurements³⁰ are in excellent agreement with our calculations. In accordance with Ref. 30 the hole pocket is absent. The results obtained for the optimized crystal structure agree better with the experimental findings than previous calculations carried out for the unrelaxed geometry. This is particularly true for the re-

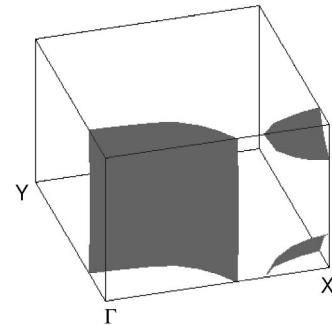


FIG. 2. Outermost Fermi surface sheet in three dimensions. In k_z direction the whole zone is shown.

gion around k_x (k_y) = $0.3 \times 2\pi/a$ touching the zone boundary. Also the chain-derived sheet moves closer to the ACAR results. This experimental feature follows the chain sheet from the zone center up to $k_x \approx 0.15 \times 2\pi/a$, transforming into the next sheet for larger k_x values. This finding is confirmed by our analysis of the atomic origin of the FS states showing predominantly chain character along this line. The only part of the theoretical Fermi surface which has not been found experimentally is the gray-shaded region in Fig. 1 stemming mostly from the chain band, but with pronounced admixture from the planes. Indeed, a big fraction of this sheet is lost when optimizing the crystal structure. This can

be seen from Fig. 2 where this outermost sheet is depicted in three dimensions. Thus we conclude that this (remaining) feature is too small in order to be detected experimentally.

In summary, a consistent LDA calculation for $\text{YBa}_2\text{Cu}_3\text{O}_7$ taking into account the relaxed crystal geometry leads to excellent agreement with experiments concerning structural data, phonons, and their pressure dependence, as well as Fermi surfaces.

This work was supported by the Austrian Science Fund, Project No. P11893-PHY. We thank the computing center of the University Graz for providing us with the vector computer facilities.

-
- ¹C. O. Rodriguez *et al.*, Phys. Rev. B **42**, 2692 (1990).
²R. E. Cohen, W. E. Pickett, and H. Krakauer, Phys. Rev. Lett. **64**, 2575 (1990).
³R. Kouba and C. Ambrosch-Draxl, Phys. Rev. B **56**, 14 766 (1997).
⁴W. E. Pickett, Physica C **289**, 51 (1997).
⁵K. Schwarz, C. Ambrosch-Draxl, and P. Blaha, Phys. Rev. B **42**, 2051 (1990).
⁶J. Kircher *et al.*, Phys. Rev. B **44**, 217 (1991).
⁷C. Ambrosch-Draxl, R. Abt, and P. Knoll, Physica C **235-240**, 2119 (1994).
⁸E. T. Heyen *et al.*, Phys. Rev. Lett. **65**, 3048 (1990).
⁹C. Ambrosch-Draxl, R. Kouba, and P. Knoll, Z. Phys. B **104**, 687 (1997).
¹⁰H. Krakauer, W. E. Pickett, and R. E. Cohen, Phys. Rev. B **47**, 1002 (1993).
¹¹O. K. Andersen *et al.*, Physica C **185-189**, 147 (1991).
¹²W. E. Pickett, H. Krakauer, R. E. Cohen, and D. J. Singh, Science **255**, 46 (1992).
¹³B. Zangger and C. Ambrosch-Draxl, Z. Phys. B **104**, 779 (1997).
¹⁴With increasing computer power, the optimization of crystal structures is becoming a standard procedure. Furthermore, regarding elastic properties one has to start from the theoretical equilibrium volume.
¹⁵R. Kouba and C. Ambrosch-Draxl, Z. Phys. B **104**, 777 (1997).
¹⁶O. K. Andersen, Phys. Rev. B **12**, 3060 (1975).
¹⁷P. Blaha, K. Schwarz, and J. Luitz, Vienna University of Technology (1997). [Improved and updated unix version of the WIEN code, published by P. Blaha, K. Schwarz, P. Sorantin, and S. B. Trickey, Comput. Phys. Commun. **59**, 399 (1990).]
¹⁸M. A. Beno *et al.*, Appl. Phys. Lett. **51**, 57 (1987).
¹⁹J. D. Jorgensen *et al.*, Physica C **171**, 93 (1990).
²⁰T. Strach, T. Ruf, E. Schoenherr, and M. Cardona, Phys. Rev. B **51**, 16 460 (1995).
²¹G. Burns, F. H. Dacol, F. Holtzberg, and D. L. Kaiser, Solid State Commun. **66**, 217 (1988).
²²K. F. McCarty, J. Z. Liu, R. N. Shelton, and H. B. Radousky, Phys. Rev. B **41**, 8792 (1990).
²³K. Syassen *et al.*, Physica C **153-155**, 264 (1988).
²⁴H. Ledbetter and M. Lei, J. Mater. Res. **5**, 241 (1990).
²⁵I. V. Aleksandrov, A. F. Gonchariv, and S. M. Stishov, Pis'ma Zh. Éksp. Teor. Fiz. **47**, 357 (1988) [JETP Lett. **47**, 428 (1988)].
²⁶M. Lei *et al.*, Phys. Rev. B **47**, 6154 (1993).
²⁷A. Bansil, Mater. Sci. Forum **175-178**, 819 (1995).
²⁸R. Liu *et al.*, Phys. Rev. B **46**, 11 056 (1992).
²⁹H. Haghghi *et al.*, Mater. Sci. Forum **105-110**, 249 (1992).
³⁰M. C. Schabel *et al.*, Phys. Rev. B **57**, 6107 (1998).